Scratch test induced shear banding in high power laser remelted metallic glass layers

Matthews, D. T. A.; Ocelik, V.; de Hosson, J. Th. M.

Published in:
Journal of materials research

DOI:
10.1557/JMR.2007.0056

Publication date:
2007

Scratch test induced shear banding in high power laser remelted metallic glass layers

D.T.A. Matthews, V. Ocelík, and J.Th.M. de Hosson[a)]
Department of Applied Physics and Netherlands Institute for Metals Research, University of Groningen, Groningen 9474 AG, The Netherlands

(Received 14 June 2006; accepted 13 October 2006)

Laser remelted surface layers of a Cu-based metallic glass forming alloy have been produced with fully amorphous depths up to 350 μm for single track widths of around 1.3 mm and have been checked by transmission of synchrotron radiation. They have been subjected to indentation hardness and scratch testing, and the development of shear bands in both situations has been addressed. During the cross-sectional hardness indentation tests, Vickers values of over 735 HV2 have been found through the depth of the treated layer, and the scratch testing has revealed extremely low friction coefficient values (<0.02 at 10 N in single-pass and 0.02 at 18 N multi-pass regimes against a diamond stylus). The shear band formation has been related to both scratch test speed (strain rate) and load (contact stress) by methods such as atomic force microscopy measurements and subsequent surface roughness characterization by a height–height correlation function.

I. INTRODUCTION

Deformation of metallic glasses has become of increasing interest in recent years, driven by a desire to better understand the formation of shear bands. A number of test methods have been utilized to develop shear bands in a controlled manner with most progress probably being found in instrumented indentation and other compression testing methods.[1–3] A significant example of such progress is that under continuous loading conditions, serrated flow associated with shear band formation is characterized by "pop-ins," or steps in load–displacement curves for particular materials, at relatively low strain rates.[1,4]

The aim of the present investigation is to study the formation of shear bands in metallic glasses; in this instance, the scratch test is the chosen test method for deformation and laser remelted surface layers provide the amorphous material. Laser remelting has previously been found to be an excellent method of fabricating thick (>250 μm) surface layers,[5] and the glass forming composition chosen was $Cu_{47}Ti_{33}Zr_{11}Ni_6Sn_2Si_1$.[6] The scratch test has long been used to analyze thin coatings and surfaces in terms of coating–substrate adhesion, friction properties, and even as a model test for abrasive wear.[7] The methodology of the test itself is straightforward, and by varying load (contact stress), pass number, pass direction, and scratch speed (strain rate), it is proposed that it will be possible to determine shear band characteristics associated with those variables.

During scratch testing, one of the outputs is sliding friction,[8] which itself is a more complex phenomenon than the classic Coulomb laws of friction may suggest. This states that, first, friction is proportional to the applied load (this proportionality is known as the friction coefficient); second, friction is not dependant upon the (apparent) applied area; and third, kinetic friction is not dependant upon the sliding velocity. In multipass scratch testing, the ploughing component has been shown to decrease in passes subsequent to the first,[9] thus leading to a reduction in friction on these passes also. Published data on multi-pass scratch testing concentrate on the failure of deposited thin films. In this paper, we address the multipass scratch test for (bulk) metallic glass investigations and investigate the development of shear bands during repetitive cycling.

II. EXPERIMENTAL PROCEDURE

Alloys were prepared by weighing the component elements and then producing an approximately 1 cm^3 "button" by arc melting. The materials are of at least 99.99% purity and in sheet, plate, pellet, or powder form prior to fabrication. The melting process is conducted in a Ti-gettered, high-purity argon (500 mbar) atmosphere. To ensure chemical and microstrucural homogeneity, the buttons are turned and remelted 3–5 times within the furnace. The buttons are then prepared for laser remelting

a)Address all correspondence to this author.
e-mail: j.t.m.de.hosson@rug.nl
DOI: 10.1557/JMR.2007.0056

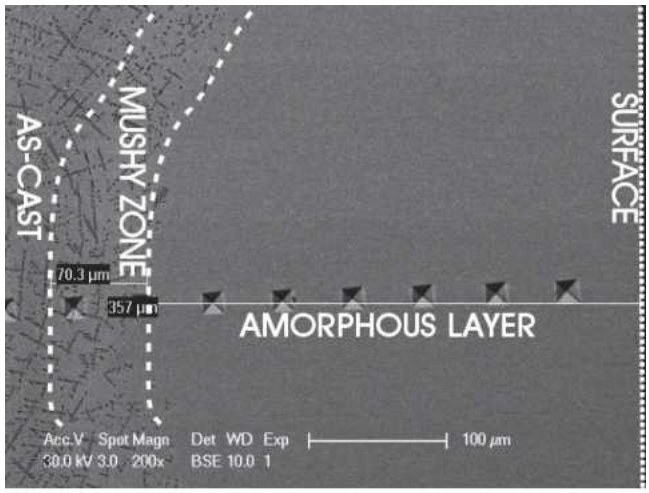

(a)

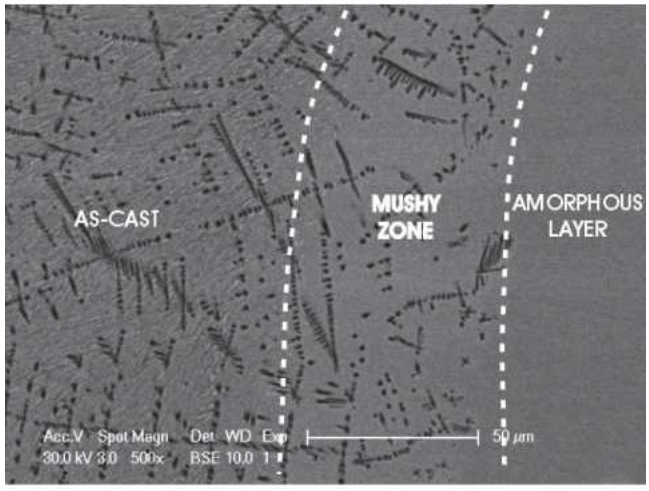

(b)

FIG. 1. (a) SEM micrograph of a Vickers hardness indented laser remelted layer, revealing the depth of the amorphous layer and (b) the mushy zone with an amorphous matrix band shown at higher magnification.

by cutting them to 15-mm-diameter hemispheres, followed by grinding and fine polishing, to produce a flat surface. Because during laser treatments some of the applied energy may be reflected, the surface is fine sand blasted to improve the absorptivity, thereby improving the efficiency of the laser processing. The laser remelting process may be conducted over a range of processing parameters, but all the data within this investigation relate to tracks remelted at a scan speed, $s = 8$ m/min and laser beam defocus $= -6$ mm, which produces a 1.3-mm-diameter laser spot with a 2 kW Rofin-Sinar Nd-YAG laser (Hamburg, Germany). The laser power is kept at 1750 W, and argon shielding of 10 l/min is always applied. All resultant arc-cast and laser processed fabrications were investigated by light microscopy, secondary electron microscopy with energy dispersive spectroscopy (SEM with EDS), (high resolution) transmission electron microscopy [(HR)TEM; FEG JEOL 2010, Tokyo, Japan] with in situ heating and electron energy loss spectroscopy (EELS) capability, and x-ray diffraction (XRD; Philips PW1710, Eindhoven, The Netherlands), and some laser tracks were investigated by synchrotron radiation on beam line ID11 at the European Synchrotron Radiation Facility (ESRF) facility (Grenoble, France). Hardness and nano-indentation examinations were conducted on a CSM Revetester (Neuchatel, Switzerland) and an MTS Nanoindenter XP (Eden Prairie, MN) with continuous strain measurement (CSM) and lateral force measurement (LFM) control, respectively, with the scratch testing being conducted on the former using a 200-µm-radius diamond Rockwell tip. The load used in the micro-indentation examinations was 2 N, while the nano-indentation was conducted to a predefined maximum load of 20 mN with a Berkovich indenter tip. Confocal optical microscopy (µSurf Nanofocus Messtechnik,

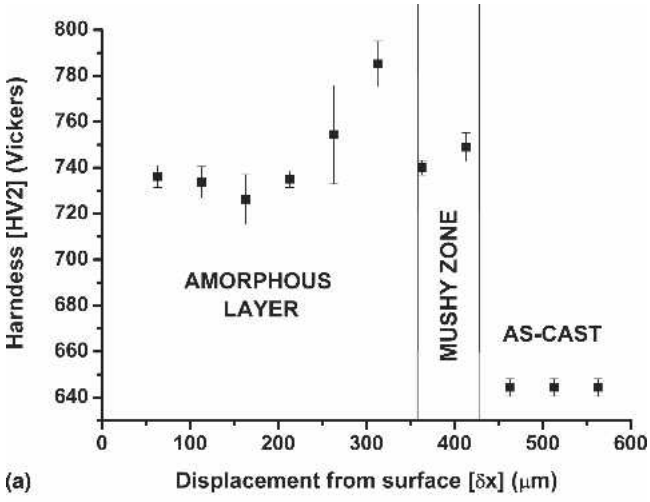

(a)

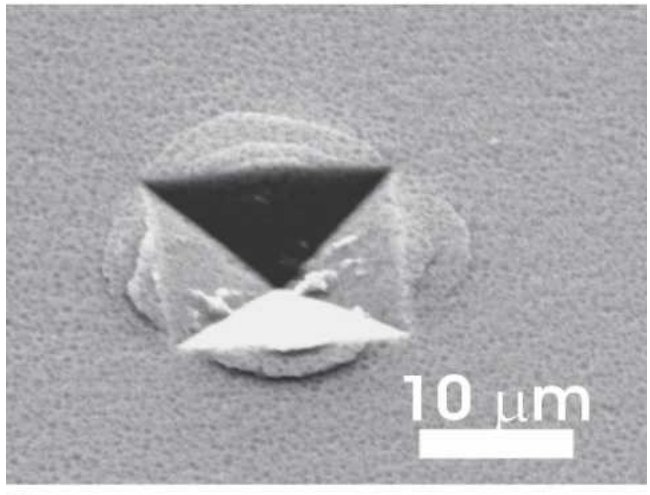

(b)

FIG. 2. (a) Vickers hardness profile from the laser remelted layer shown in Fig. 1 and (b) a microindent revealing peripheral damage caused during indentation in the region near the substrate-coating interface leading to pileup.

Duisburg, Germany) and tapping-mode atomic force microscopy (AFM; Digital Instruments Dimension 3100 Atomic Force Microscope, USA) were additionally implemented in the characterization of the scratch grooves and the worn surfaces. To analyze the AFM and confocal microscopy, a MATLAB code was written and implemented with the aim to calculate height–height correlation functions.

III. RESULTS AND DISCUSSION

A. Microstructural characterization and hardness profile

Laser remelted layers have been characterized as amorphous by light microscopy, XRD, synchrotron radiation, SEM, and TEM. It is shown in Fig. 1(a) that the depth of a typical fully amorphous layer is 350 μm, with a further 70-μm amorphous matrix layer with retained Ti dendrites [shown in more detail in Fig. 1(b)] being attributed to a "mushy zone" in which the close-to-eutectic matrix readily forms a glassy structure, with the Ti dendrites being more stable and therefore retained within the amorphous matrix. The width of this track is 1.3 mm. For this remelted layer, the hardness is found to be quite high (>735 HV2) over the full depth, width, and length of the coating. Figure 2(a) shows a cross-sectional hardness profile through a laser remelted layer. There are some notable deviations in the hardness values through the coating depth. This is associated with shear band formation and sometimes cracking (and therefore stress release) in some indentations. It was observed that the highest hardness indentations showed the most peripheral deformation, caused by residual stress relaxation. Upon release of these stresses, the material may "relax" to apparently lessen the indent volume, thus showing "higher hardness" when assessed by the standard "bird's eye" surface measurement. Another contribution may come from the fact that during laser remelting, a residual stress profile is usually formed with a high tensile component near the surface, which gradually turns to a compressive component close to, or into the substrate.[10] This may be seen in the rise in hardness close to the substrate [Fig. 2(a)] and a microindentation taken from this region in Fig. 2(b) exhibiting peripheral shear band formation. Hardness indentations as recorded by nanoindentation showed the material to have a hardness of around 13 GPa and an elastic modulus of around 130 GPa. The discrepancy in hardness values compared

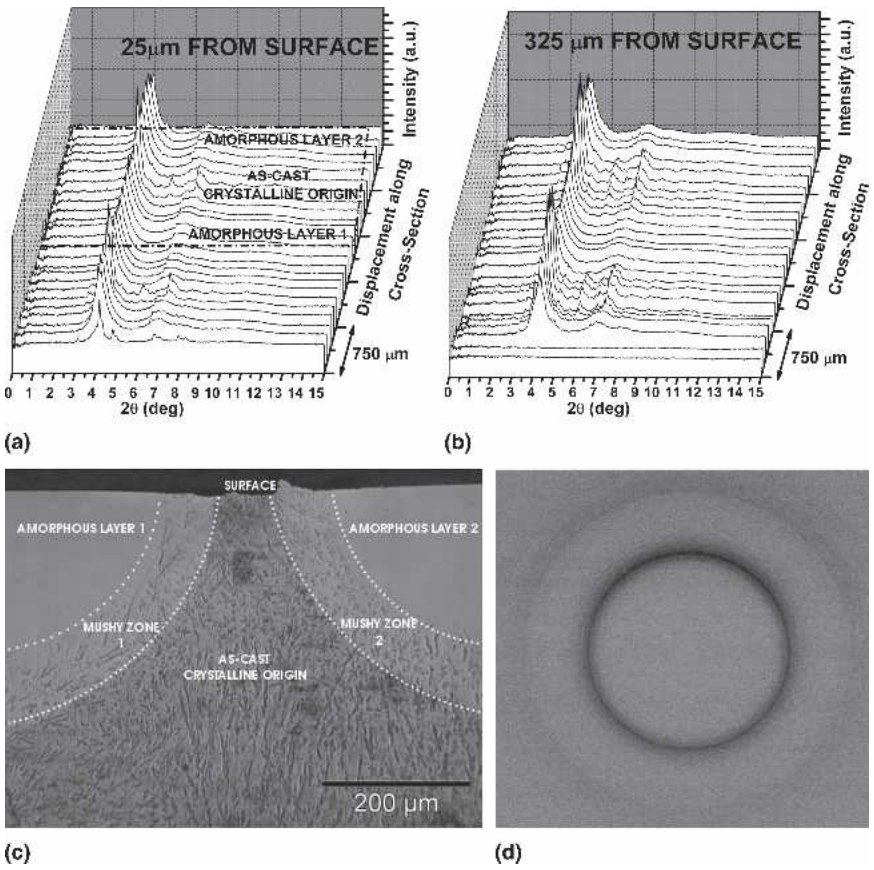

FIG. 3. 2θ plots from transmission synchrotron radiation results of adjacent laser remelted tracks calculated by integration of 2D signal from (d): (a) across the top of the layers, (b) close to the base of the layers, (c) optical micrograph showing the area highlighted by the dash-dot parameter in (a), and (d) a diffused diffraction ring attained through a track center on 2D digital camera detector.

with the Vickers test may be due to the smaller indent size in the nanoindentation test, which may influence the relative importance of shear band formation. The effect on an amorphous material may be even more important with regard to the interaction of developed and developing shear bands during indentation. These were seen in both indentation modes, but there was greater evidence of the shear band formation in the Vickers tests.

B. Synchrotron characterization

While the layers appear "featureless" in light and secondary electron microscopy, it is not sufficiently conclusive to determine whether the layers are fully amorphous. Synchrotron radiation is a source of high energy radiation, which may be considered in much the same way as a XRD, except the x-rays are generated with much lower wavelength and higher intensity.[11] This tool is beneficial in two ways. Due to the very high intensity and penetration depth of a synchrotron beam, relatively thick samples may be characterized, thus making it an ideal tool for longitudinal characterization of laser tracks. The result can be seen in standard 2θ or two-dimensional (2D) powder diffraction patterns. The synchrotron beam was produced with 80.4 keV, giving a working wavelength of 0.15422 Å, administered with a "spot" area of 30 μm × 20 μm.

The results in Figs. 3(a) and 3(b) show data for one full track and (portions of) two adjacent tracks, divided by the as-cast crystalline material. The test method is so powerful that it is in fact possible to map the area in and around the tracks to determine the transition from amorphous to amorphous matrix "mushy zone," to crystalline material, and this is plotted in the 2θ graphs. The humps around 4° in Figs. 3(a) and 3(b) may be considered to be related to an amorphous halo. The crystalline area becomes larger and more pronounced as the depth is increased and relates to an area such as the "as-cast crystalline origin" area shown in Fig. 3(c), which relates to the area outlined by a dotted box in Fig. 3(a). The diffused diffraction ring, attained through the center of the track [Fig. 3(d)], confirms that the laser tracks are amorphous. The sample–detector distance was 217.84 mm, and the detector size was 10 cm × 10 cm. The image shown in Fig. 3(d) has been cropped for clarity, but the center of the broad band corresponds to the broad peak in Figs. 3(a) and 3(b), which equates to a *d*-spacing of 1.104 Å ($\theta = 4.01°$).

C. Scratch results

In tribological contacts, it is often desirable to reduce friction between two contact surfaces. With the scratch test, it is possible to evaluate the friction properties for a given contact regime. In the chosen regime, that contact involves a 200-μm-radius diamond ball being indented into, and slid across, a surface at a given normal load and scratch speed. The method of applying this load may be varied incrementally or progressively, or applied constantly. This investigation is concerned with the latter two test modes.

1. Progressive loading

The progressive load scratch test results (Fig. 4) revealed that the friction of metallic glasses obeys classic laws and increases with increasing load linearly until unstable deformation occurs, at which point the friction rises significantly and fluctuates until the entire contact is governed by material smearing (high adhesion). At loads below this severe deformation, the friction coefficient of the laser treated layers is extremely low (0.03–0.04 for single-pass tests between 7 and 20 N loads), although it is also evident that at loads below 5 N, the contact is not stable enough to return consistent results, and the friction coefficient is therefore seen to fluctuate until a stable contact is developed (Fig. 4). The progressive single-pass test also provided an easy method for determining the load required to develop surface-visible shear bands (~10 N) and the point at which this shear band development transforms into unstable deformation and consequently material smearing (~28 N). The inset images (A)–(E) in Fig. 4 attempt to highlight these areas more clearly. Inset A shows the initiation of surface-visible shear bands in the scratch base; inset B reveals this shear band formation to be stable. Inset C indicates the transition to material smearing within the contact, which is accompanied by higher friction (0.12); inset D exhibits a second, relatively stable regime, in which the friction rises linearly before extensive edge shear band formation

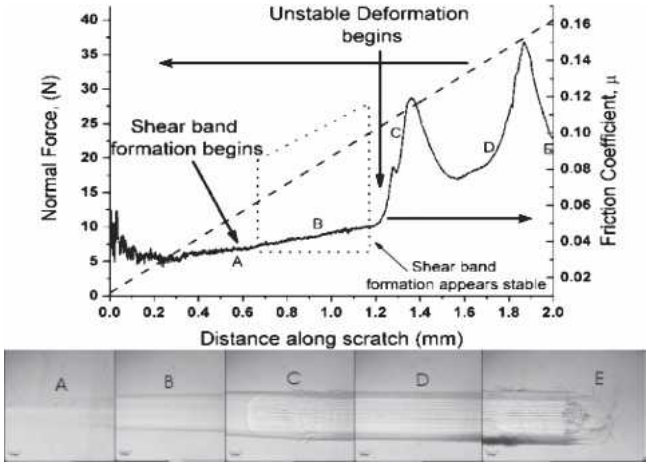

FIG. 4. Scratch output curve revealing the effect of progressive loading on the friction coefficient between 0.4 and 40 N over a displacement of 2 mm. (A–E) correspond with those areas identified in the curve for (A) onset of shear banding, (B) stable shear band forming region, (C) onset of unstable deformation, (D) apparent material smearing, and (E) the end of the scratch.

occurs (seen in inset E), leading to a second rise in the friction coefficient to 0.15.

Fully crystalline samples of the same composition have been tested in progressive and constant loading, and the friction resolved is on the order of 0.7 at 18 N loads. The crystalline state of the material tested consisted of a eutectic matrix, with needles and dendrites therein. Thus, it was far from an equiaxed grain structure, but crystalline nonetheless. The material was found to be smeared through the scratch, leading to a high adhesion in the contact, which leads to the high friction coefficient. Multi-pass testing was not deemed necessary in these samples since material transfer to the diamond stylus and subsequent increased material smearing radically altered the loading in repeated scratches.

2. Varying scratch speed

In accordance with classical friction laws, amorphous metals are seen not to be significantly affected by varying speed with respect to changes in friction coefficient. This is shown in Fig. 5(a); confocal microscopy confirmed that the track depth and width are also not adversely affected by scratch speed over the prescribed test range [Fig. 5(b)]. However, the height of the pileup region seems to increase with increasing scratch speed. Some contrast was seen in the scratch base, which took the form of apparent shear banding in all samples under optical microscopy investigations. Confocal microscopy itself was not sufficient to resolve these features, but further analysis will be shown later.

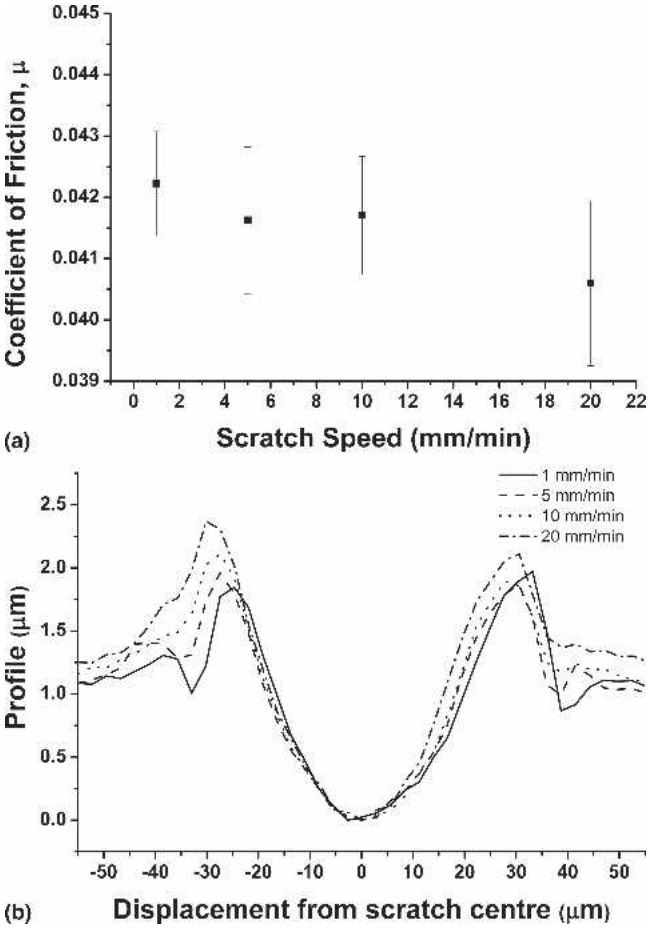

FIG. 5. (a) Graph showing the average friction coefficient and its standard deviation versus scratch speed with (b) showing the profiles for the differing speeds.

3. Multi-pass scratch testing

Given that the scratch speed plays no significant role in the friction coefficient value, an arbitrary value of 5 mm/min was chosen for the multi-pass scratch testing, and the load was chosen to be 18 N, from the progressive load tests (Fig. 4), as this load was found to be beyond that necessary to initiate shear banding in the track base but below that which induces shear-banding within the pileup region. The friction results for an increasing pass number are shown in Fig. 6, together with analysis by confocal microscopy conducted on the multipass samples, which determined the track width and depth. The spread in the width and depth data that is not seen in the friction data is purely statistical spread. The results for the friction were recorded simultaneously and plotted as such, leading to a "true representation" over one series of passes. The width and depth data are taken from individual tracks subjected to 1, 2, 4, 5, 7, and 10 passes, since the technology was not available to measure the track depth and width in situ. The fit and trend are still remarkable and in no way invalidate the observations following.

These results reveal an exponential-type decay with increasing pass numbers for the friction coefficient, which was found to continue for up to 300 pass numbers, while the depth and width data somewhat mirror this behavior. This observation is complimentary to similar experiments conducted on thin films; however, of course

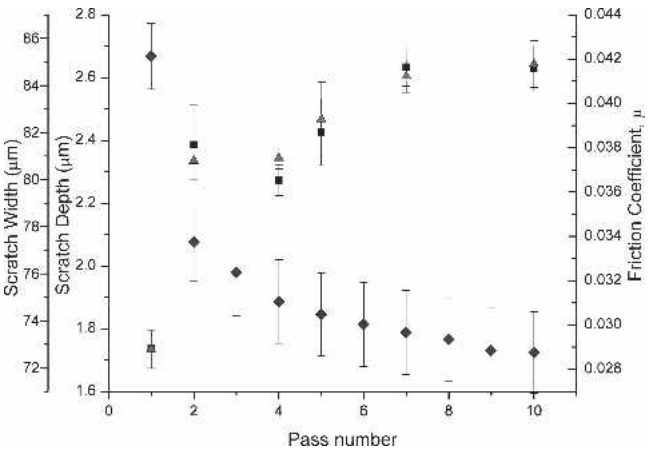

FIG. 6. Graph revealing the dependence of scratch width (triangles), track depth (squares), and average friction (diamonds) on the pass number.

in the current investigation, no "failure of the coating" (by spalling for example) can occur as would be seen by thin deposited coatings.

It is now generally accepted that the friction coefficient ($\mu = F_T/F_N$), where F_T is the tangential force and F_N is the normal (applied) force, is made up of two components, an adhesion component μ_a (related to the interfacial friction coefficient μ_s) and a ploughing component μ_p. It follows that this reduction in friction coefficient may be attributed to two factors. In our case, the ploughing component of friction is reduced with increasing pass numbers in a nonlinear manner, and the contact area is also reduced, which would also lead to a reduction in the adhesion component. An interesting phenomenon develops in metallic glasses during scratch testing, however, which may, in part at least, contribute toward the reduction in friction coefficient, and this is a surface roughening of the scratch base, induced through the development of shear bands.

The scratches themselves may be observed macroscopically with confocal microscopy, and Fig. 7 shows a typical result; here the three-dimensional (3D) image is of the center of a scratch attained at 5 mm/min sliding speed, with a load of 18 N after 10 repeated passes. Shear bands developed in the groove created by the motion of the indenter are not visible with confocal microscopy, but steps created by shear band development within the pileup are clearly resolved.

The confocal microscopy method of surface profiling, however, is not powerful enough to resolve the fluctuations involved with shear band formation on the scale developed during scratch testing for single pass and low pass numbers (<20 passes). AFM is, however, able to do this, and it has therefore been utilized in tapping mode to characterize the topography of the scratch and to analyze the height and distribution of the scratch surface in the direction of the scratch test. It can be seen in Fig. 8 that the formation of shear bands on the side of the scratch groove can be clearly identified by AFM. The average height of a shear band formed under single-pass conditions at 25 N load and 1 mm/min speed is 5–10 nm, and the angle of the shear band formation with respect to the scratch direction is found to be approximately 45°; however some deviation from an exact "straight line" was seen [Figs. 8(a) and 8(b)].

FIG. 7. 3D confocal micrograph taken at the midpoint of a scratch subjected to 10 scratch repetitions with scratch speed = 5 mm/min and normal load = 18 N.

4. Shear band identification with the height–height correlation function

For increasing pass numbers, it was observed that the profile of a scratch base was significantly changed. This is shown in Fig. 9, where the selected profiles along the sides of the scratch grooves of samples tested at 1, 5, and 10 passes are shown. To attain a better understanding of this change, it was considered appropriate to approach the surface roughness observations using height–height correlations as the investigative tool. An understanding of the height–height correlation function is assumed in this paper, but a more complete explanation of the method may be found elsewhere.[12] The height–height correlation function $H(r)$ is given by Eq. (1) for an isotropic, self-affine surface where L is the whole measured length with the profile $h(x)$ along that length

$$\langle H(r)\rangle_L = \frac{1}{L}\int_{-L/2}^{L/2}[h(x+r) - h(x)]^2 dx \quad . \qquad (1)$$

Using this method enables the acquisition of several independent parameters, namely α [roughness (or Hurst) exponent; the gradient of the graph $= 2\alpha$], and this essentially gives an indication of the correlation, w [root-mean-square (rms) roughness], and ξ (the lateral correlation length). As a cautionary note, it should be realized that three important assumptions were made during this investigation: first that the method of investigation was done so as an isotropic surface; second, that that implies a self-affine surface[12]; and third, that any change in surface roughness may be attributed to the development formation of shear bands. A surface subjected to scratch testing, which in turn induces shear bands, is clearly an anisotropic surface. However, given that the data were analyzed only in the so-called "fast scan" direction (the x direction in the AFM images), it is reasonable to assume the surface in this is isotropic, since this relates to the scratch direction and the shear-band density/formation over a given range, which is expected to be isotropic. This was confirmed by fitting a Fourier transform over the profile.

The height–height correlation itself was calculated in the area of interest, determined from the AFM images; the surface height data were exported, read into a simple MATLAB code, and fed into the mathematical code for analysis by Eq. (1).[12] The data were leveled by removing the parabolic and linear components of the profile along

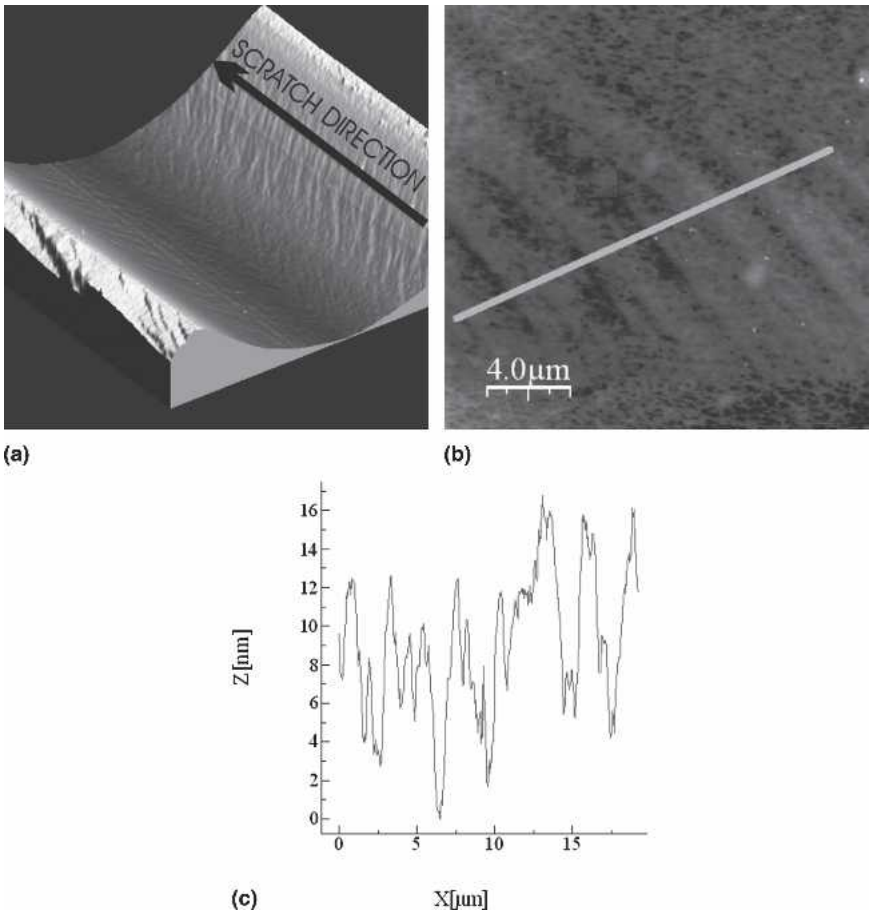

FIG. 8. (a) 80 μm × 80 μm AFM image for a laser remelted track submitted to 10 scratch passes, (b) 20 μm × 20 μm AFM image for a 1 mm/min single-pass scratch test clearly showing shear band formation, and (c) the leveled profile along the line perpendicular to the shear bands.

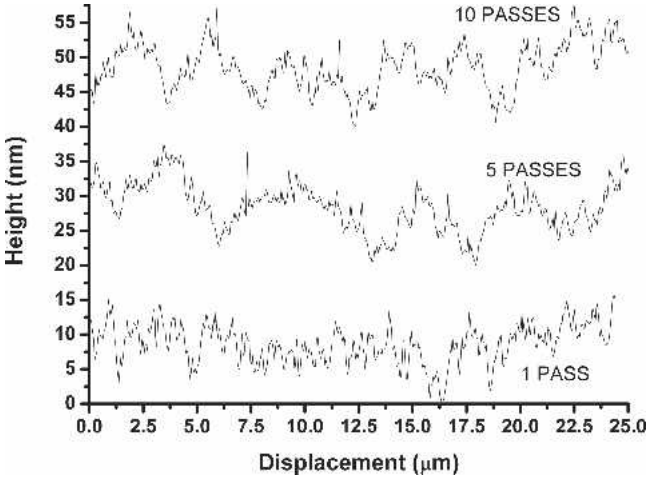

FIG. 9. AFM scratch profiles for 1, 5, and 10 passes revealing clear differences between the 3 tests.

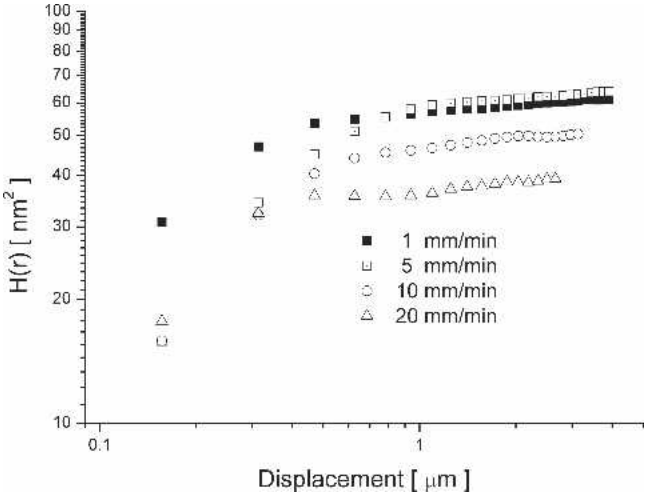

FIG. 10. Graph revealing the height–height correlation function of single-pass scratch tests conducted at differing scratch speeds.

the scan direction, which was calculated by fitting the profile to a second-order polynomial equation.

When this method is applied to varying scratch speed (Fig. 10; it is reasonable to relate this to varying strain rate, which is cited as very important in shear band development),[1,13] one sees a characteristic slope 2α for linear behavior at low displacements. The root mean square (rms) roughness w, characterized by the saturation

value $H(r) = 2w^2$ for displacements larger than the correlation length ξ, appears to reduce with increasing strain rate. The correlation length ξ also decreases with increasing strain rate. The correlation length ξ is defined as the intersection of the lines associated with 2α and $2w^2$ (if they are extrapolated to meet each other; see Fig. 11). This may be expected and shows that faster strain leads to a denser shear banding characteristic. The reduction in ξ is found to reduce from 0.6 for 1 mm/min scratch speeds down to 0.38 for 20 mm/min scratch speeds.

Figure 11 attempts to highlight the important results in height–height correlation function analysis. The height–height correlation of surfaces subjected to varying pass numbers exhibits two regimes. The graph itself shows data obtained from AFM measurements for a polished surface: a 1-pass scratch and a scratch subjected to 30 passes. The final rms roughnesses were found to be very similar (around 7.2 nm for 30 passes and 6.7 nm for 1 pass). As can be seen in Fig. 11, the curve for 30 passes exhibits 2 different gradients before saturation is achieved whereas the as-polished surface and the 1-pass sample exhibit only 1 gradient (and therefore 1 value for α). For those samples having two gradients, the intersection of the second gradient with the $2w^2$ line is considered to be important. The first gradient α_1 is found to be characteristic of the development of initial shear banding on a small correlation length, and a second gradient, which relates to larger length scales, is classified here as α_2.

When the increase in α_1 is considered, a relationship is seen, which, after an initial reduction with respect to the polished surface, is around 0.35 for up to 10 passes, but which then increases for pass numbers larger than this to a value of around 0.65. This is then found to be constant, for up to 100 passes, signaling an increase that somewhat mirrors the behavior seen in the reduction in friction coefficient, in that after some time, a steady state is reached. The second gradient α_2 was found to begin after 5 passes and reveals an initially linear increase between 0.184 for 5 passes up to 0.3 for 20–30 passes, which then plateaus for pass numbers greater than 20–30 at this value of around 0.3. This mirrors somewhat the trend seen in the friction coefficient.

The correlation length was also seen to follow an interesting trend in that it also reached a plateau for pass numbers greater than 5. This typical value of ξ was found to be 2 μm, which relates to the inter-shear spacing (defined here as the distance between the end of one shear band and the start of the next in the x direction) of shear band development (Fig. 8). For lower numbers of scratches, the correlation length was found to be 0.5–0.6 and may be related to the initiation of shear banding as it correlates with the ξ values found for single-pass scratch tests subjected to varying scratch speed. This is a very interesting result and implies that the development of shear bands may contribute (albeit not necessarily proportionally) to the reduction in friction. This is to say that the reduction in friction coefficient is positively affected by the development of shear bands (not the roughness developed by the shear bands). In fact, the extremely low friction coefficient seen in the current investigation may be attributed to the shear band formation in metallic glasses, which in turn facilitates slip within the material and a low internal friction coefficient, which, as stated previously, is a governing factor in the adhesion component of friction.

5. High value pass numbers

When the number of passes is increased, the same trend in the reduction of the friction coefficient is seen (Fig. 12). The data shown here are for 100 passes and are again exponential in appearance. At around 70 passes, the friction coefficient becomes apparently stable, or

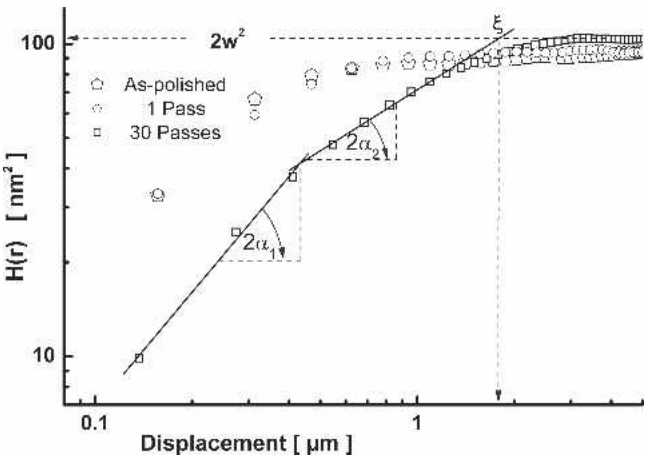

FIG. 11. Graph showing height–height correlation functions for varying numbers of passes conducted at 5 mm/min scratch speed.

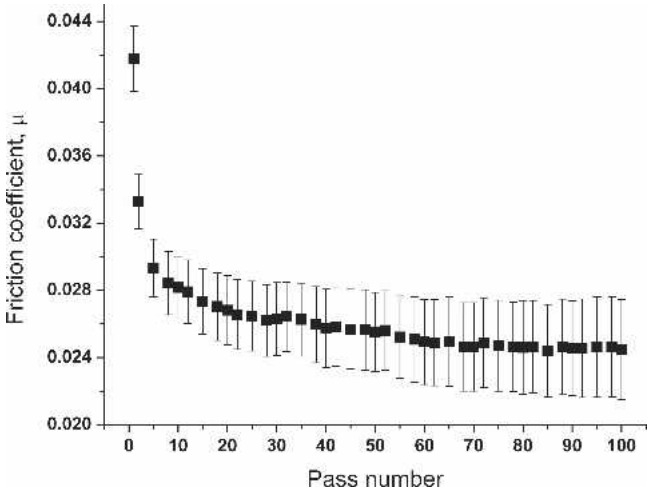

FIG. 12. Friction coefficient as a function of pass numbers for 100 passes.

saturated, which implies that the contact becomes optimum. Even with further passes, there is little change in the friction (after 300 passes, the average friction coefficient was still only 0.027); however, to aid clarity, the associated data are not shown here.

It was also found that the growth of the shear bands becomes increasingly prevalent and can even be measured by confocal microscopy analysis [Figs. 13(a) and 13(b)] and seen with SEM [Fig. 14(a)]. Figure 13(a) highlights the difficulty of analyzing the development of shear bands for low numbers of passes (in the figure this is 10 passes). However, for larger pass numbers (100 and 300), the shear band growth (in height) is clearly seen. At this scale, the shear band height rises from 5–10 nm, for low pass numbers, up to 60–70 nm. A second very interesting observation is that the frequency (density) of the shear bands does not increase, which implies that the development of shear bands is localized and remains so through repetitive scratching, with only an increased amplitude. This in accordance with results from the height–

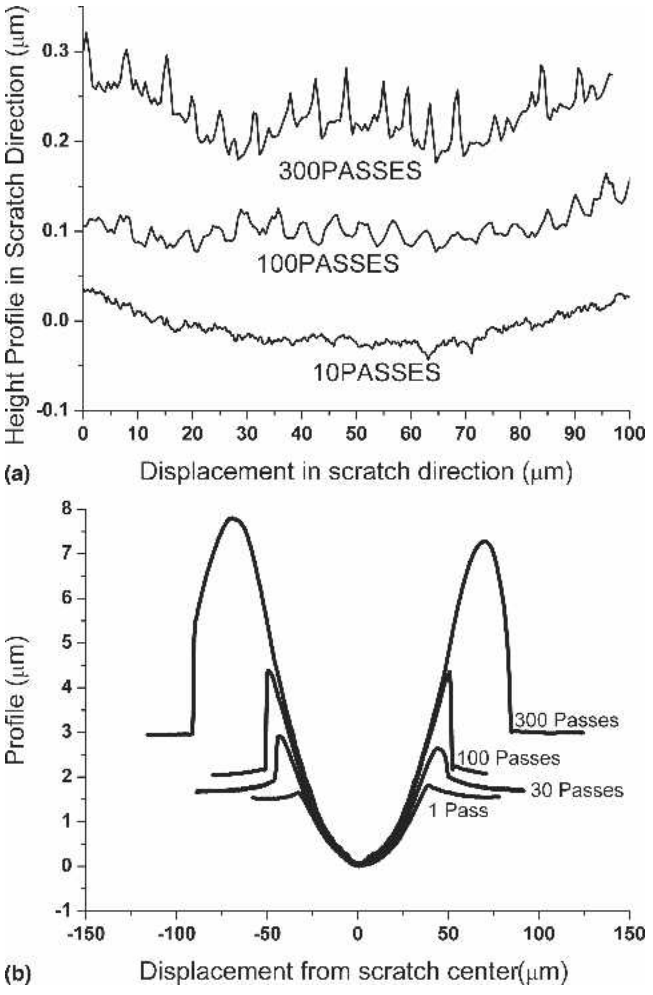

FIG. 13. (a) Confocal microscopy profiles for 10, 100, and 300 passes taken in the scratch direction, with (b) revealing the track width and depth dependence on the number of passes.

height correlation data, and AFM analysis was undertaken to confirm the more "local" density of the shear banding, and indeed confirmed the observation seen through confocal microscopy. A possible explanation for this is the fact that no work-hardening occurs in amorphous materials. Therefore, once a shear band has been produced, the material in it is softer than the original amorphous material. The displacement between these shear bands may then be governed by the indenter tip geometry, which affects the stress field. This is of course consistent during dynamic testing in terms of repetition, and therefore, these two factors together mean that the shear bands produced originally sustain all further deformations.

Figure 13(b) reveals the change in scratch geometry of increasing pass numbers. Considering the earlier fact that the friction reached a steady state, even though the width and depth continue to increase, and the error, or fluctuation in the friction showed a steady increase, the indication is that while the magnitude of the macroscopic ploughing component continues to decrease, the increased surface roughness induced through the formation of the shear bands counterbalances this on a micro- or nanoscale. Therefore, while the formation of shear bands is beneficial in the reduction of the friction coefficient, their own development hinders further reductions in the friction coefficient.

Pileup induced through repetitive scratch testing appears, on first impressions, to be radically increased at larger pass numbers. An interesting observation is seen with regard to the "real" appearance of the pileup. At low pass numbers, the pileup is seen to take the form of a shear band and is maintained as part of the sample, which "rises" with increasing pass numbers. Figure 14(a) shows the difference in scratch appearance with increasing pass numbers. The scratch direction is shown in Fig. 14(a), and areas of shear banding are highlighted in the three scratches. After 100 passes, the shear bands are found to aggregate somewhat, and further scratch passes "push" the material out of the scratch, which then forms a lip. A clearer representation of this development is shown in Figs. 14(b)–14(d). The fact that a lip is formed, however, is important in the analysis because the depth and width data reported incorporate the pileup at the edge of the track. This is valid where the pileup is in direct contact with the deformed material and a direct result of shear banding. The formation of lips, which are not in contact with the scratch itself, cannot be considered representative of the shear banding in the same way and varies wildly depending on the chosen area of investigation. In this instance, it is better to define the depth and width with respect to the original surface. The cracking in the lips is considered to form due to the release of stresses in the lip.

Rather remarkably, the easiest identification of the

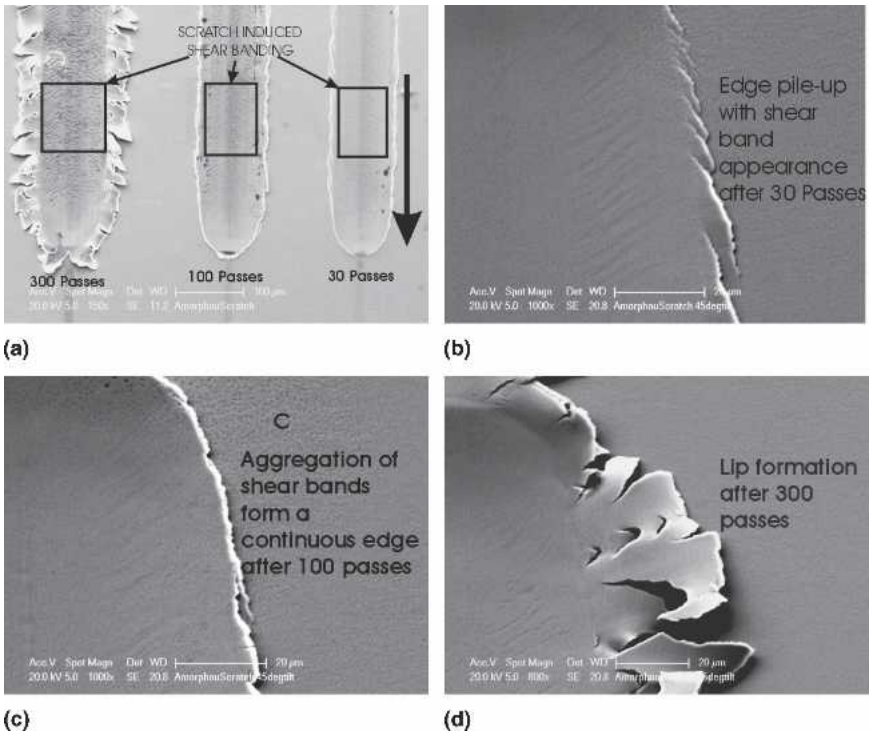

FIG. 14. SEM micrographs revealing (a) comparison of the track appearance after 30, 100, and 300 passes, with higher magnification micrographs showing the development of edge pileup for (b) 30 passes, (c) 100 passes, and (d) 300 passes.

scratch base after 300 passes was retrieved from the optical microscope of the scratch tester. Figure 15 clearly shows how the shear bands develop in three separate regions, identified as "shear zones." Zones 1 and 3 in the figure at the top and bottom of the track (effectively the scratch "sides") reveal shear bands formed at approximately 45° to the scratch direction (the axis of maximum shear stress) as expected for amorphous materials; however, along the base of the scratch, the shear banding appears to form perpendicular to the scratch direction in a 30-μm band. The lip formation at the track edge is also visible, and there appears to be a characteristic spacing between deformation within this lip of around 20–30 μm, which may be related to cracking or a consequence of the initial shear band formation and its continued growth.

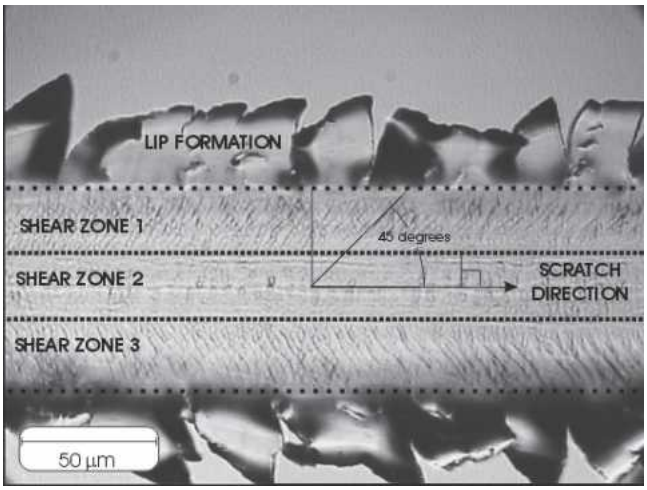

FIG. 15. Light microscopy micrograph from the center of a laser remelted track subjected to 300 repetitive scratches exhibiting edge lip formation, and 3 shear zones along the scratch base.

IV. CONCLUSIONS

Laser remelting has been shown to be an excellent method of attaining thick (>350 μm) amorphous layers on the surface of glass-forming alloys. This is due to the locally high cooling rates attainable by this processing route. Characterization of these layers has been achieved through transmission of synchrotron radiation, which has proved to be a powerful technique in the analysis of such layers regarding their amorphous nature, and their hardness has been found to be >735 HV2 over the full depth and length of the layers.

Unidirectional scratch testing in progressive load single pass, varying speed at constant load single pass, and constant load multi-pass modes has been investigated to develop a controlled formation of shear bands, and results reveal that metallic glasses exhibit exceptionally low friction coefficients (<0.04 at single-pass 20 N loads) until material smearing dominates the contact induced by high loading (>35 N), at which point the friction rises sharply as the adhesion component of the friction coefficient dominates the contact regime. In accor-

dance with classical friction laws, no noticeable dependence of the friction coefficient on the scratch speeds used was noted. The scratch depth and width follow the same trend under these conditions. Application of the height–height correlation function to varying scratch speed does, however, reveal that surface roughness (attributed to shear band development) is reduced, as is the lateral correlation length (down to 0.38 at 20 mm/min), implying that the increase in scratch speed increases the density of shear bands. This relates well to classical theories regarding the effect of strain rates on inhomogeneous flow in metallic glasses.

An interesting phenomenon was witnessed in the friction coefficient due to multipass sliding contact in metallic glasses, in that it appears to follow an exponential decay with increasing pass numbers, which reduces to an average value of 0.027 for large pass numbers. The scratch track depth and width both mirror this behavior, implying that the friction coefficient is somewhat dependent upon the ploughing component. The scratch base was analyzed with AFM, and a change in scratch profile appearance was seen. This was attributed to the development of shear bands in the scratch and, to analyze this, the surface roughness was characterized by the height–height correlation function. Analysis of the roughness exponent α revealed one stage at low pass numbers and two stages at higher pass numbers. This was mirrored by the behavior of the lateral correlation length ξ, which increased to a plateau of 2 μm, which is the shear band interspacing. Because no increase in these attributes was seen with increased pass numbers, this shows that the densification of shear bands is independent of the pass numbers for pass numbers greater than 10 but the increase in shear band height is dependent on the number of cycles.

Longer pass numbers confirm these observations and reveal that the amorphous layer remained "intact" for over 300 passes. No catastrophic failure or material smearing was seen during testing, and this was mirrored in a remarkably low coefficient of friction even after 300 passes. The scratch surface after such a number of passes is shown to develop three "shear zones." These form on the scratch sides and in the base. The first two reveal "conventional" shear band development with surface steps at approximately 45° to the scratch direction, while the latter shear band development steps are seen to be perpendicular to the scratch direction.

An interesting development was also witnessed with respect to the edge pileup. This was seen to begin with an appearance akin to shear band formation. These shear bands are then found to be pushed away from the scratch with increasing pass numbers to such a point that they aggregate and form a uniform edge. With increasing pass numbers, this transforms to a lip formation, which is no longer in direct association with the material surface. This is then found to crack upon release of the stresses built up during the formation of this lip.

ACKNOWLEDGMENTS

The authors acknowledge financial support from the Foundation for Fundamental Research on Matter (FOM-Utrecht) and the Netherlands Institute for Metals Research (NIMR).

REFERENCES

1. C.A. Schuh and T.G. Nieh: A nanoindentation study of serrated flow in bulk metallic glasses. *Acta Mater.* **51,** 87 (2003).
2. S. Jana, U. Ramamurty, K. Chattopadhyay, and Y. Kawamura: Subsurface deformation during Vickers indentation of bulk metallic glasses. *Mater. Sci. Eng., A* **375–377,** 1191 (2004).
3. A.V. Sergueeva, N.A. Mara, J.D. Kuntz, E.J. Laernia, and A.K. Mukherjee: Shear band formation and ductility in bulk metallic glass. *Philos. Mag.* **85,** 2671 (2005).
4. B. Yang, L. Riester, and T.G. Nieh: Strain hardening and recovery in a bulk metallic glass under nanoindentation. *Scripta Mater.* **54,** 1277 (2006).
5. D.T.A. Matthews, V. Ocelik and J.Th.M. de Hosson: Metallic glass layers produced by high power lasers, in *Bulk Metallic Glass. Special Issue, Mater. Sci. Eng. A* (in press).
6. E.S. Park, H.K. Lim, W.T. Kim, and D.H. Kim: The effect of Sn addition on the glass-forming ability of Cu–Ti–Zr–Ni–Si metallic glass alloys. *J. Non-Cryst. Solids* **298,** 15 (2002).
7. S.J. Bull and D.S. Rickerby: Multi-pass scratch testing as a model for abrasive wear. *Thin Solid Films* **181,** 545 (1989).
8. B.N.J. Persson: Sliding friction. *Surf. Sci. Rep.* **33,** 83 (1999).
9. S. Bennett, A. Matthews, A.J. Perry, J. Valli, S.J. Bull, and W.D. Sproul: Multi-pass scratch testing at sub-critical loads. *Tribologia. Finnish J. Tribol.* **13,** 16 (1994).
10. M. Pilloz, J.M. Pelletier, and A.B. Vannes: Residual stresses induced by laser coatings: Phenomenological analysis and predictions. *J. Mater. Sci.* **27,** 1240 (1992).
11. *Third Generation Hard X-ray Synchrotron Radiation Sources: Source Properties, Optics, and Experimental Techniques,* edited by D.M. Mills (Wiley, USA, 2002).
12. Y. Zhao, C.C. Wang, and T.M. Lu, *Characterization of Amorphous and Crystalline Rough Surface: Principles and Applications* (Academic Press, Elsevier, USA, 2001).
13. F. Spaepen: A microscopic mechanism for steady state inhomogeneous flow in metallic glasses. *Acta Metall.* **25,** 407 (1977).